Available online at www.sciencedirect.com
SCIENCE DIRECT
ACADEMIC PRESS
Journal of Sound and Vibration 267 (2003) 509–522
JOURNAL OF SOUND AND VIBRATION
www.elsevier.com/locate/jsvi

Extended validation of a theoretical model for railway rolling noise using novel wheel and track designs

C.J.C. Jones*, D.J. Thompson

Institute of Sound and Vibration Research (ISVR), University of Southampton, Highfield, Southampton SO17 1BJ, UK

Accepted 9 May 2003

Abstract

A theoretical model for railway rolling noise, TWINS, was first developed some years ago and was previously validated against field measurements for conventional wheel and track designs. This model has subsequently been used in the design of noise-reducing wheels and tracks. An outcome of the recent Silent Freight and Silent Track projects was a series of novel designs that were tested in a comprehensive field experiment. Alongside this development, the theoretical model has been updated to improve accuracy and include new features. The results of 34 wheel/track combinations that were measured in field experiments are compared with corresponding predictions using the improved model. It is found that the mean difference between measured and predicted overall A-weighted sound pressure levels is less than 2 dB while the standard deviation is 1.9 dB. The improved accuracy of the model is also shown by a reanalysis of the original validation experiments.

1. Introduction

Rolling noise is usually the dominant source of environmental noise arising from the operation of trains. This is radiated from the wheels of the vehicle and from the track, which vibrate during rolling because of the roughness of the wheel and rail surfaces. Wheels and track can be designed to reduce the noise and a theoretical model to enable such design work has been developed and used extensively [1]. The Track–Wheel Interaction Noise Software (TWINS) is a suite of programs that allows rolling noise emission from railway wheels and tracks to be calculated based on their respective designs [2]. A series of experiments was performed in 1992/3 in which the TWINS software was validated for a number of conventional situations [2,3]. A total of 25 combinations of wheel, track and train speed were investigated, made up of 3 wheel types, 3 track types and up

*Corresponding author. Tel.: +44-2380-593-224; fax: +44-2380-593-190.
E-mail address: cjcj@isvr.soton.ac.uk (C.J.C. Jones).

doi:10.1016/S0022-460X(03)00711-9

to 4 speeds, although not all possible combinations were considered. Since then, a number of projects have used TWINS in design studies that lead to wheels and tracks that differ substantially from those considered in the validation tests. In particular, some of the designs developed within the Silent Freight and Silent Track projects [4] are beyond the scope of the original validation.

The combined final tests in 1999 of the Silent Freight and Silent Track projects [4] now provide measurement data that allow this validation to be extended. In particular, a number of novel designs have been included in these tests, themselves the results of design studies using TWINS. These new designs embody a greater range of values of various important parameters and it is therefore important that the validation should be extended from conventional situations to include these novel designs. This should allow the model to be used with greater confidence in future design studies.

Since the validation of 1992/3 [2,3], made with TWINS version 2.2, a number of modifications have been made to the model to improve the accuracy and the scope. Relevant improvements include the following. (1) A model of the sleeper allowing for its modal behaviour is included. The frequency-dependence of the ballast stiffness is also included. It has not been possible to use this model in the present work although it is now fully available. (2) The wheel radiation model has been improved [5]. The main difference is in the component of sound produced by the radial motion of the wheel. (3) The rail radiation model has been improved to take better account of three-dimensional effects at low frequencies and at high decay rates [6]. (4) The sound pressure calculations include a model for the ground reflections that allows for a frequency-dependent complex ground impedance. (5) It has been observed that no peak associated with the radial mode with one nodal diameter is seen in measured wheel receptances on the vehicle. This is due to the influence of the axle. However, a practical solution to correct the model is to set the damping loss factor of this mode to 1 to eliminate its effect. This practice has therefore been adopted.

Because of these changes, it is also necessary to confirm that the validation carried out previously still applies to the updated software, TWINS 3.

2. Field experiments

Table 1 lists the track and wheel designs that were tested in 1999. Fuller details of these can be found in Ref. [4]. The test track was built in three sections. Section 1 was kept as the reference track A. Tracks B–F were constructed by modifying sections 2 and 3 during the test. This gives a total of 36 combinations of wheel and track (34 excluding the modified 920 mm wheel without damping rings). These have been tested for only a single speed, 100 km/h, and, in each case, a single roughness condition, though the roughness of each track section and each wheel differ slightly.

3. Modelling the situations in the field tests using twins

3.1. Modelling the wheels

To model wheels in TWINS, a finite element free vibration analysis is first required. This was carried out using an axisymmetric analysis in proprietary finite element software. Only the wheel

Table 1
Track and wheel designs that were tested in the Silent Freight/Silent Track experiment

Tracks	Wheels
(A) Reference track (UIC60 rail on monobloc sleepers with soft studded rubber pads).	(1) Reference wheel (UIC 920 mm diameter standard freight wheel).
(B) Reference track fitted with tuned absorbers.	(2) Modified 920 mm wheel with ring dampers.
(C) As track A but with stiffer pads.	(3) 860 mm wheel AD860F[a] with perforated web and ring dampers.
(D) As track C but fitted with tuned absorbers.	(4) 860 mm wheel ISVR860F[a] with web shields.
(E) New build track (rail section with narrow foot, new rail fastener system, optimised bibloc sleepers).	(5) 860 mm wheel ISVR860F[a] with tuned absorbers.
(F) As track E but fitted with tuned absorbers.	(6) Wheel 3 with ring dampers removed[b].
	(7) Wheel 5 with tuned absorbers removed[b].
	(8) Wheel 2 with ring dampers removed[b].

[a] AD860F and ISVR860F are each designs of wheel derived within the Silent Freight project with 860 mm diameter.
[b] Tested only on tracks A and E.

was modelled, this being constrained at the inner edge of the hub. The finite element analysis provides a list of natural frequencies and mode shapes at key positions. This must be augmented with modal damping ratios for each mode. For lightly damped wheels, the modal damping ratios are not required to be known precisely. In the current analysis, however, some of the wheels have added damping treatments. In these cases it is important that the correct level of damping is included in the model. As part of the field tests, limited modal analysis of each wheel was performed. Thus, measured modal damping ratios have been obtained for each wheel and these damping values were used in the modal parameter data.

The position of the wheel/rail contact on the wheels varied slightly between wheels. In determining the wheel receptances, however, it was taken as 83 mm from the flange-back in all cases.

For wheel 4 with web shields, two modal parameter files were tested. The first takes the amplitudes on the shields to be equal to those on the wheel web at the corresponding radius (worst case). The second takes the amplitudes on the shields to be zero (best case); i.e., it assumes that noise from the web is screened to such an extent that it becomes an insignificant contributor to the total wheel noise and that radiation from the shield itself is also insignificant. A complete model of the web shields would have to take into account the transmission through the shield of the acoustic radiation from the web, the effect of the acoustic cavity behind shield and the radiation of the shield itself due to its own vibration response to excitation via its mounting to the wheel. Such a model has not been implemented within the scope of the current work. The second method of modelling described above has therefore been used to produce the results presented here. No account is taken therefore of the amplification that is seen in measured vibration on the shield compared to the web at low frequencies. It has been assumed that this does not contribute to the wheel noise significantly because of the low radiation efficiency associated with the thin, flexible material of the shield.

In order to model wheel 3 with a perforated web, the finite element model is based on a wheel with a solid web but a correction to the radiation efficiency has been used.

3.2. Modelling the tracks

Several different track models are available in TWINS. For the purposes of the current study, the tracks have been modelled using only the simplest of these models. This represents the track as a Timoshenko beam resting on a continuous foundation of two layers of damped springs between which is a layer of mass corresponding to the sleepers. The parameters used for the tracks are summarized in Table 2. Important parameters in defining the track vibration are the pad stiffness, the decay of vibration with distance along the track and the level of coupling between vertical and lateral motion. The pad and ballast stiffnesses and damping values were selected by comparing predictions of track accelerances with static measurements made on the test tracks.

Table 2
Track parameters

	Tracks A and B	Tracks C and D	Tracks E and F
Rail	UIC60	UIC60	Narrow foot
Vertical bending stiffness EI_v	$6.42 \times 10^6\,\mathrm{N\,m^2}$	$6.42 \times 10^6\,\mathrm{N\,m^2}$	$6.24 \times 10^6\,\mathrm{N\,m^2}$
Shear coefficient κ_v	0.4	0.4	0.4
Loss factor η_{rv}	0.025	0.030	0.022
Lateral bending stiffness EI_l	$1.07 \times 10^6\,\mathrm{N\,m^2}$	$1.07 \times 10^6\,\mathrm{N\,m^2}$	$0.96 \times 10^6\,\mathrm{N\,m^2}$
Shear coefficient κ_l	0.4	0.4	0.4
Loss factor η_{rl}	0.010	0.010	0.015
Mass per unit length ρA	60.3	60.3	56.0
Cross receptance factor L_k	-11 dB	-11 dB	-11 dB
Coupling sign	+1	+1	+1
Integration length L	14 m	14 m	14 m
Pad	Reference pad	Stiffer pad	New fastener
Vertical stiffness K_{pv}	$8.0 \times 10^7\,\mathrm{N\,m^{-1}}$	$2.2 \times 10^8\,\mathrm{N\,m^{-1}}$	$1.0 \times 10^8\,\mathrm{N\,m^{-1}}$
Loss factor η_{pv}	0.16	0.25	0.12
Lateral stiffness K_{pl}	$1.6 \times 10^7\,\mathrm{N\,m^{-1}}$	$3.0 \times 10^7\,\mathrm{N\,m^{-1}}$	$4.0 \times 10^7\,\mathrm{N\,m^{-1}}$
Loss factor η_{pl}	0.16	0.25	0.12
Sleeper	Conventional monobloc	Conventional monobloc	New bibloc
Model[a]	'bibloc'	'bibloc'	'bibloc'
Half sleeper mass m_s	140 kg	140 kg	100 kg
Sleeper spacing D	0.6 m	0.6 m	0.6 m
Half length L	1.25 m	1.25 m	0.95 m
Ballast			
Vertical stiffness K_{bv}	$5.0 \times 10^7\,\mathrm{N\,m^{-1}}$	$5.0 \times 10^7\,\mathrm{N\,m^{-1}}$	$5.0 \times 10^7\,\mathrm{N\,m^{-1}}$
Loss factor η_{bv}	1.0	1.0	1.0
Lateral stiffness K_{bl}	$3.5 \times 10^7\,\mathrm{N\,m^{-1}}$	$3.5 \times 10^7\,\mathrm{N\,m^{-1}}$	$2.0 \times 10^7\,\mathrm{N\,m^{-1}}$
Loss factor η_{bl}	1.0	1.0	1.0

[a] 'bibloc' indicates the sleeper is represented purely as a mass.

In predicting the noise, the decay of vibration with distance along the track can be either predicted or adjusted in the model according to measured data. The latter procedure was adopted in Ref. [3] and found to give more reliable results than using predicted decay rates. For the tracks fitted with absorbers, a considerable increase in decay rate is observed above about 400 Hz for both vertical and lateral directions compared to the same track without absorbers. Thompson et al. [7] discusses predictions for the decay rates of rail with the absorbers and compares them with the measurements. Here, calculations for the damped tracks are based entirely on the decay rates measured during the tests. The vertical and lateral measured decay rates for each of the tracks of Table 1 are presented in Fig. 1. In these graphs the decay rates with and without the tuned absorbers are compared for each of the three basic track sections.

The decay rates were measured with the track unloaded. Such decay rates are of primary relevance for noise prediction since most of the effectively radiating length of rail is far enough away from the wheel loads. However, a small effect on the noise level may be expected for rail pads that have a great change of stiffness under load since this raises the decay rates in the track locally at each wheel load position. An analysis of this effect is reported in Ref. [8]. However, no such analysis has been carried out in the scope of the present work.

The coupling between lateral and vertical motion is determined by the cross-receptance of the track (and that of the wheel). In the track model this is determined from the vertical and lateral receptances by a single factor L_k. This has been set to -11 dB on the basis of the observed ratio of lateral rail vibration to vertical rail vibration.

3.3. Other parameters

The train speed is set to 100 km/h and the wheel load to 35 kN as in the tests. The ground is modelled using a frequency-dependent impedance defined by a typical flow resistivity value.

In the tests three microphone positions are used to sample the noise radiation at a radial distance of 3 m from the nearer rail head; $L_{p,A}$ level with the rail head, $L_{p,B}$ at an elevation of 22.5° and $L_{p,C}$ at an elevation of 45°. The calculation is therefore carried out for the same three positions. In both the measured and predicted case, the levels are combined into a single weighted estimate of sound pressure, $L_{p,ABC}$:

$$L_{p,ABC} = 10\log_{10}\{0.4 \times 10^{(L_{p,A}/10)} + 0.2 \times 10^{(L_{p,B}/10)} + 0.4 \times 10^{(L_{p,C}/10)}\}.$$

this follows the practice of the 1992 tests [2,3] and provides an averaged measure of the noise radiated at angles relevant to environmental noise propagation. It is a more stable measure for comparison than single microphone position measurements, which would be sensitive to small variations in the directivity of the radiation.

3.4. Analysis of the roughness

Within TWINS, a roughness-processing model that is referred to as the distributed point-reacting springs (DPRS) model [9] has been used. This takes roughness measurements made on a series of parallel lines on the surface of the wheel (or rail) and calculates, for each position around the wheel (along the track), an equivalent single roughness height. This allows for the flexibility of

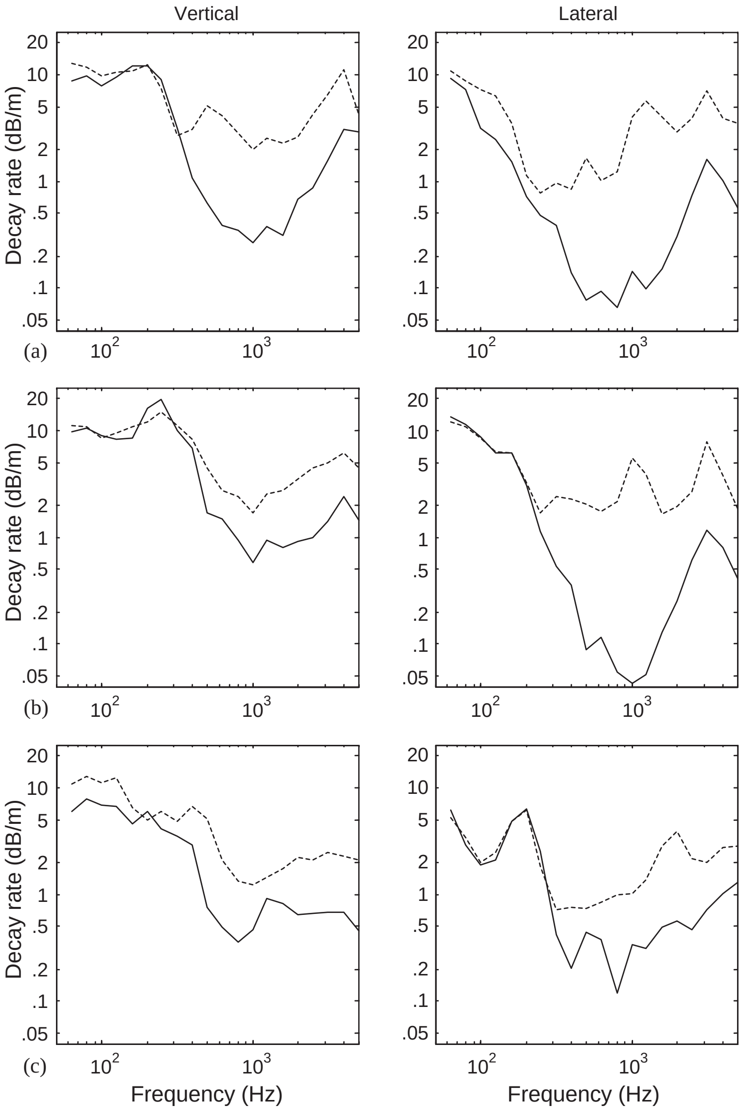

Fig. 1. Decay rates measured in the 1999 field tests for each track section (Table 1). (a) A and B, (b) C and D and (c) E and F; —— track without tuned absorbers (A, C and E), - - - - track with tuned absorber (B, D and F).

the contact patch and its finite size in both the length and width directions, i.e., contact filtering and correlation effects across the contact patch.

For each test section of track, detailed rail roughness measurements were made on the near rail on three lengths of 1.2 m, overlapping by 0.2 m. In each case these covered 11 parallel lines with a spacing of 2.5 mm between lines.

Detailed measurements were also made of the roughness of the test wheels. However, these measurements have been found to be flawed at short wavelengths due to instrumentation noise. Since the wheels were all in new condition and, for the purpose of the test, unbraked, the wheel roughnesses were generally low and below those of the rails. The wheel roughness has therefore not been used in the calculations which are therefore based only on the rail roughness. The error introduced by ignoring the wheel roughness may cause an under-prediction but this is be expected to be small.

4. Results of the validation for the 1999 field tests

4.1. Noise predicted from roughness

Fig. 2 compares predicted and measured noise in terms of overall A-weighted levels. The individual points each represent one of the 34 wheel/track combinations. The solid line corresponds to the mean difference between prediction and measurement (which is -1.7 dB). The dashed lines show a range of $\pm$one standard deviation, which is 1.9 dB. From this graph it can be seen that the overall trends are predicted correctly, although in some instances the discrepancy between individual points and the mean line is up to 3.5 dB. Moreover, there are individual cases where a situation is measured as quieter than another, but predicted as noisier. There is a 10 dB range in the noise levels presented. This is due to the performance of the various prototypes all assessed at one train speed. Details of the performance of the different prototypes are given in Ref. [4]. In the 1992 experiments there was a 25 dB range in noise levels that was due to the range of train speed and roughness.

To illustrate the spectral variations, the difference between predicted and measured noise spectra is constructed for each of the 34 cases. Fig. 3 shows the mean and a range of $\pm$one

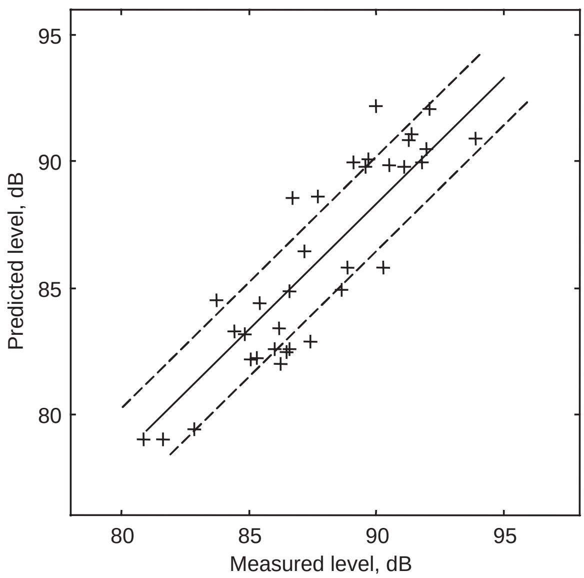

Fig. 2. Predicted overall A-weighted sound pressure level for measured decay rates compared to measured level. + results for 34 wheel/track combinations, —— mean, - - - one standard deviation range.

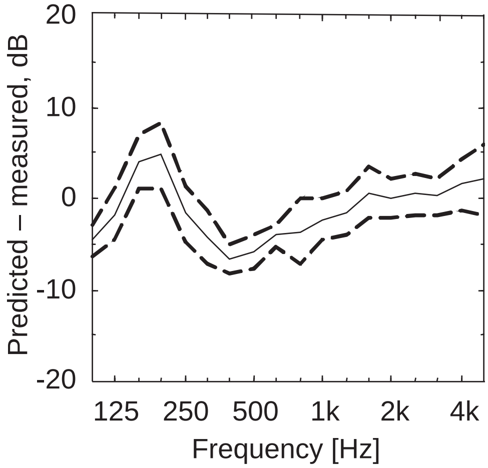

Fig. 3. Predicted sound pressure level for measured decay rates minus measured level, averaged over 34 wheel/track combinations, —— mean, - - - one standard deviation range.

standard deviation of these difference spectra. The result can be seen to be generally close to 0 dB, with an over-prediction at low frequencies (around 200 Hz) and an under-prediction around 400 Hz. The reasons for these features is the inadequacy in the modelling of the sleeper vibration (which is the dominant source at these frequencies), as will be discussed further below. Use of the modal sleeper model and hence the frequency-dependent ballast stiffness model would greatly improve the predictions in this frequency region.

The standard deviation of these results is mostly 2–3 dB, which is smaller than found in earlier validation tests, where it was 3–5 dB [3]. The reason for this is that the roughness, and in particular the position of the contact patch, is more closely controlled in the current experiments.

In order to indicate the influence of the measured decay rates on the above results, Fig. 4 shows the A-weighted levels obtained using predicted decay rates, again plotted against the corresponding measured levels. Only the results for the three tracks without added damping are shown, since no attempt is made here to predict the effects of the absorbers. Compared with the earlier results in Fig. 2, the mean line is similar, but the standard deviation of the results is reduced from 1.9–1.1 dB.

In an attempt to simulate the effects of the modal sleeper model, a prediction has been performed in which the ratio of sleeper vibration to rail vibration is made equal to the measured ratio. This modifies only the noise radiated by the sleeper. The result is shown in Fig. 5. Compared to Fig. 3, the shape of the response is improved and the peak at 200 Hz has been eliminated. However, the predicted level seems too low for all frequencies below 1 kHz. This has been found to be due to inadequacies in the rail vibration level predicted by this calculation.

4.2. Noise predicted from measured vibration

In order to study the radiation part of the model in isolation, it is desirable to predict noise from measured vibration. Unfortunately, there are too few measurement points for this. In order to overcome this, the predictions are first carried out in the normal way, and the separate

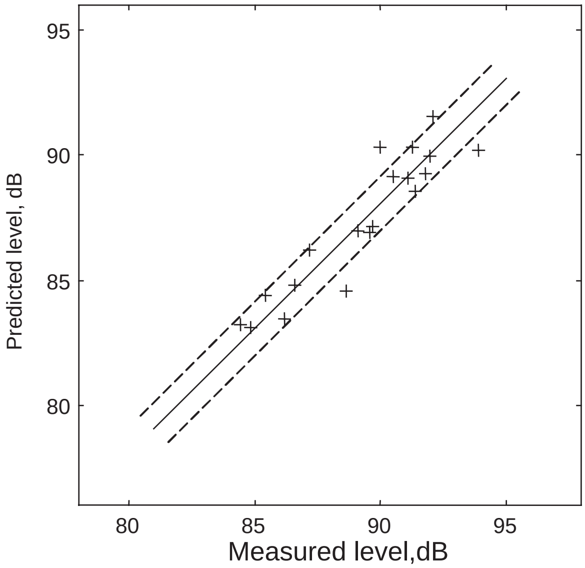

Fig. 4. Predicted overall A-weighted sound pressure level compared to measured level for predicted decay rates (only for tracks A, C, E). + results for 19 wheel/track combinations, —— mean, - - - one standard deviation range.

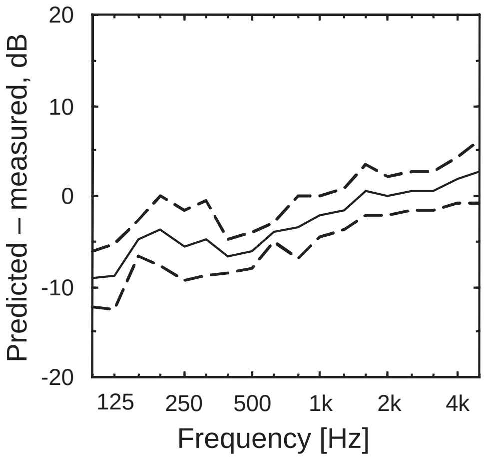

Fig. 5. Predicted sound pressure level for measured decay rates and measured sleeper/rail vibration ratios minus measured level, averaged over 34 wheel/track combinations, —— mean, - - - one standard deviation range.

components of sound (due to wheel axial vibration, wheel radial vibration, rail vertical vibration, rail lateral vibration and sleeper vertical vibration) are obtained. These are then multiplied by the ratio of measured to predicted vibration applying in each case and then re-assembled to give an estimate of the total sound pressure. Since, the wheel vibration was measured on track Section 1, which has slightly higher roughness than the other sections, a roughness correction is applied to this in adjusting the wheel component of sound.

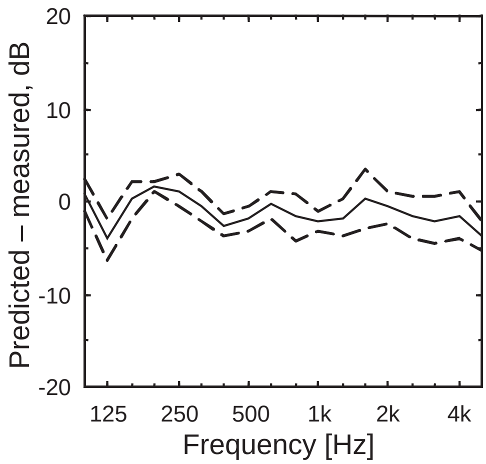

Fig. 6. Predicted sound pressure level from measured vibration minus measured sound pressure level, averaged over 34 wheel/track combinations, —— mean, - - - one standard deviation range.

The spectral results of noise predicted on the basis of the measured wheel and rail vibration spectra are shown in Fig. 6. Compared with the full prediction (Fig. 3), this has a mean line which is more consistently close to 0 dB, and a smaller variation (standard deviations of 1.5–2 dB). This reinforces the reliability of the radiation predictions that was found in the 1992 validation exercise [3]. Moreover, the introduction of a better ground model in the sound pressure level prediction has clearly improved the spectral form of these results compared to the earlier validation [3].

The results of predicting noise from measured vibration are plotted in Fig. 7 in terms of overall A-weighted level against the corresponding measured level. Compared to the earlier results of Fig. 2, the predictions based on measured vibration appear slightly more consistent. The standard deviation is 1.6 dB whereas it was 1.9 dB previously. On average, the predicted level is 1.0 dB below the measurements in this case (compared to 1.7 dB in Fig. 2).

5. Reanalysis of the previous validation cases

The validation tests of 1992 [2,3] involved three wheel types, each of diameter 920 mm—an SNCF Corail wheel, an SBB EW-IV wheel, with doubly curved web, and a DB 'optimized' wheel. Three track types were also tested—an SBB track with UIC54 rail, concrete bibloc sleepers and stiff rail pads, a second SBB track, with UIC54 rail and wooden sleepers, and a DB track with UIC60 rail, concrete monobloc sleepers and medium stiffness rail pads. Tests were carried out at 80, 125 and 160 km/h. At the two SBB sites the DB wheels were not available so a fourth speed of 50 km h^{-1} was added. This gave a total of 25 combinations.

For each of these combinations new predictions have been performed using TWINS 3. The same parameter values are used as in the previous validation study. As before, the measured decay rates are used and the sound pressure level is predicted as the weighted average of three positions at 3 m from the near rail and different heights. The predicted and measured levels are plotted in Fig. 8.

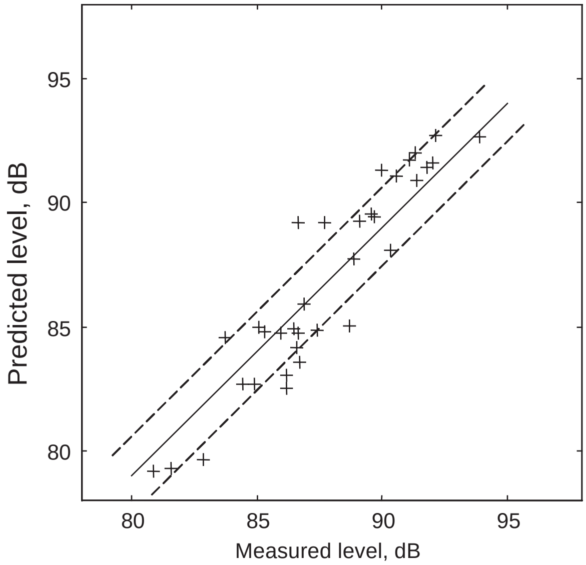

Fig. 7. Predicted overall A-weighted sound pressure level from measured vibration compared to measured level. + results for 34 wheel/track combinations, —— mean, - - - one standard deviation range.

The predictions are on average 2.7 dB higher than the measurements, and the standard deviation of the differences is 2.0 dB (which is similar to that found in Section 4 above). These results are little changed from those obtained using TWINS 2.2 [3]. As previously, the worst agreement is found for the DB optimized wheel for which it was suspected that the roughness measured after the tests was atypical of that applying during the tests [3].

The spectral results are summarized in Fig. 9. For comparison, the results from Ref. [3], obtained with TWINS 2.2, are shown in Fig. 10. The mean line in Fig. 9 now contains less systematic fluctuation. In particular, the under-prediction below 250 Hz and over-prediction around 500 Hz in Fig. 10 have been rectified by the inclusion of the new ground reflection model. At high frequencies the wheel radiation has been increased slightly.

The standard deviation of these differences is dominated by uncertainties in the roughness. Nevertheless, the results for TWINS 3 in Fig. 9 have an average standard deviation of 3.9 dB compared to 4.6 dB in the results for TWINS 2.2, with an improvement particularly noticeable for the most important frequency range of 500–2000 Hz.

In summary, compared with the previous validation test results, TWINS 3 is shown to give similar agreement in terms of A-weighted level, and improved agreement in terms of spectra.

It is not thought to be justified to combine the results of the new (1999) validation tests with those of the 1992 tests since they were performed on different bases. In particular, in the 1992 tests the roughnesses and transverse profiles of the wheels and rails were in service condition, whereas in the 1999 tests they were specially conditioned.

Nevertheless, it is interesting to note that the 1992 tests conclude that the prediction of the noise is on average 2–3 dB too high, whereas, in the present tests, it is concluded that the predictions are on average 1–2 dB too low. This may be due to the use of the rail roughness without the wheel

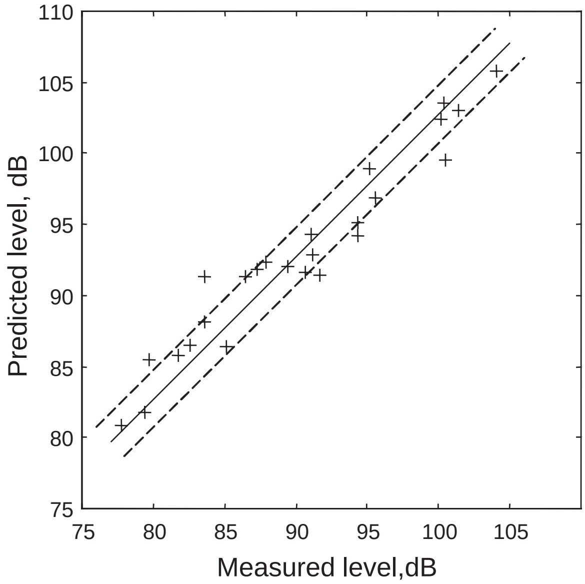

Fig. 8. Predicted overall A-weighted sound pressure level for measured decay rates compared to measured level. + results for 25 wheel/track/speed combinations from 1992 validation tests, —— mean, - - - one standard deviation range.

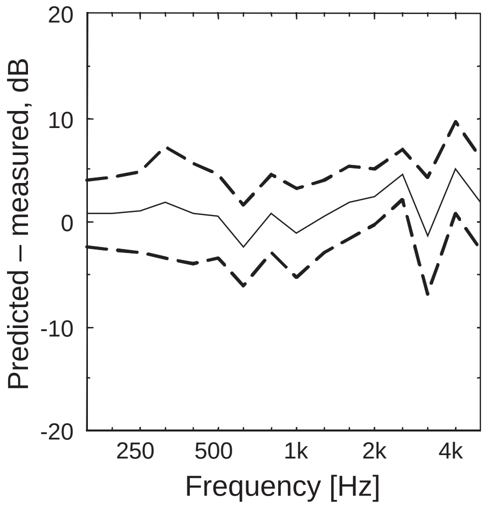

Fig. 9. Predicted sound pressure level from TWINS 3.0 for measured decay rates minus measured level, averaged over 25 wheel/track/speed combinations from 1992 validation tests, —— mean, - - - one standard deviation range.

roughness. Another factor which may influence this difference is that the 1992 tests were performed on passenger vehicles which have significant shielding of the wheels on the far side of the vehicle. The present tests were performed on freight vehicles for which this shielding effect is minimal. This could have an influence of up to 2 dB.

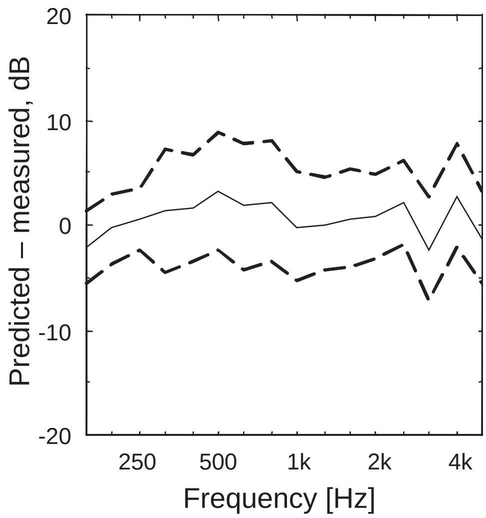

Fig. 10. Predicted sound pressure level from TWINS 2.2 for measured decay rates minus measured level, averaged over 25 wheel/track/speed combinations from 1992 validation tests, —— mean, - - - one standard deviation range.

6. Conclusions

The revised TWINS software has been shown to give improved predictions of sound pressure level due to rolling noise from trains. The wheel roughness measurements were not used as they were contaminated by measurement noise. Since the wheels were all in new condition and unbraked, the wheel roughnesses were generally low and below those of the rails. The effect is therefore expected to be small but may have contributed to the general under-prediction of the sound level. However, the difference between measured and predicted noise is less than 2 dB while the standard deviation is 1.9 dB. This reduces to 1.1 dB when the track decay rates are based on prediction instead of measurement. Predictions would also be improved by using the modal sleeper model but this was not operational in the version of TWINS 3 in use.

The range of situations available in the 1999 tests gives a good selection of new noise reduction technologies (e.g., rail and wheel damping) but only a small range of other parameters such as pad stiffness, rail shape and track structure; on the other hand, the 1992 tests contained a wider range of track structures, pad stiffness and measurements were made for a range of train speeds.

TWINS has been shown to predict the noise radiation correctly for the combined measurement at the three, 3 m microphone positions that were used in the tests; the noise predicted from measured vibration agreed very well with measured noise.

Acknowledgements

This work has been undertaken as part of the Silent Freight and Silent Track projects funded by the European Union (Brite Euram projects BE 95-1238 and BE 96-3017, contract numbers BRPR-CT95-0047and BRPR-CT96-0258).

References

[1] D.J. Thompson, C.J.C. Jones, A review of the modelling of wheel/rail noise generation, *Journal of Sound and Vibration* 231 (2000) 519–536.

[2] D.J. Thompson, B. Hemsworth, N. Vincent, Experimental validation of the TWINS prediction program for rolling noise, Part 1: description of the model and method, *Journal of Sound and Vibration* 193 (1996) 123–135.

[3] D.J. Thompson, P. Fodiman, H. Mahé, Experimental validation of the TWINS prediction program for rolling noise, Part 2: results, *Journal of Sound and Vibration* 193 (1996) 137–147.

[4] B. Hemsworth, P.-E. Gautier, R. Jones, Silent Freight and Silent Track projects, *Proceedings of Internoise 2000*, Nice, France, 2000, pp. 714–719.

[5] D.J. Thompson, C.J.C. Jones, Sound radiation from a vibrating railway wheel, *Journal of Sound and Vibration* 253 (2) (2002) 401–419.

[6] D.J. Thompson, C.J.C. Jones, N. Turner, Comparison of 2D and 3D rail radiation models, ISVR Contract Report 99/28, 1999.

[7] D.J. Thompson, C.J.C. Jones, T.P. Waters, The development of a tuned damper for reducing noise from railway track, *Structural Dynamics: Recent Advances, Proceedings of the Seventh International Conference.* Southampton, 2000, pp. 567–578.

[8] D.J. Thompson, C.J.C. Jones, T.X. Wu, G. De France, The influence of non-linear stiffness behaviour of rail pads on the track component of rolling noise, *Proceedings of the Institution of Mechanical Engineers, Part F* 213 (1999) 233–241.

[9] P.J. Remington, J. Webb, Estimation of wheel/rail interaction forces in the contact area due to roughness, *Journal of Sound and Vibration* 193 (1996) 83–102.